NACA RM L50G13a

NACA

RESEARCH MEMORANDUM

INVESTIGATION AT TRANSONIC SPEEDS OF A 35-PERCENT-CHORD AILERON ON A TAPERED WEDGE-TYPE WING OF ASPECT RATIO 2.5 WITH AND WITHOUT A FUSELAGE

By Thomas R. Turner and Joseph E. Fikes

Langley Aeronautical Laboratory
Langley Air Force Base, Va.

NATIONAL ADVISORY COMMITTEE
FOR AERONAUTICS

WASHINGTON
September 8, 1950

NACA RM L50G13a

NATIONAL ADVISORY COMMITTEE FOR AERONAUTICS

RESEARCH MEMORANDUM

INVESTIGATION AT TRANSONIC SPEEDS OF A 35-PERCENT-CHORD AILERON ON A TAPERED WEDGE-TYPE WING OF ASPECT RATIO 2.5 WITH AND WITHOUT A FUSELAGE

By Thomas R. Turner and Joseph E. Fikes

SUMMARY

An investigation at subsonic and transonic speeds has been made in the Langley high-speed 7- by 10-foot tunnel to determine the effects of fuselage diameter on some of the aerodynamic characteristics of an unswept wing having a 6-percent-thick modified double-wedge section, an aspect ratio of 2.5, and a taper ratio of 0.625 with a 35-percent-chord aileron. Two fuselages were investigated in conjunction with the wing. The small fuselage had a maximum diameter of approximately 20 percent of the wing span and the large fuselage had a maximum diameter of approximately 40 percent of the wing span. The investigation covered a Mach number range from 0.60 to 1.18 with the Reynolds number varying from 9.6×10^5 to 1.2×10^6.

The addition of either of the two fuselages investigated in conjunction with the wing had practically no effect on the lift-curve slope of the wing investigated and did not seriously affect the aileron effectiveness.

INTRODUCTION

The use of low-aspect-ratio wings to alleviate the adverse effects of speed has led to the problem of designing controls for such wings, particularly when they are used in conjunction with relatively large fuselages. Although design charts are available for calculating the control characteristics of wings of relatively low aspect ratio at subsonic speeds (references 1 and 2), the question of what wing dimensions to use in the calculations becomes of importance; that is, should the exposed part be considered as the wing or should the wing be considered as extending through the fuselage. As part of the NACA general transonic program, studies are being made to determine the effect of fuselage size on the characteristics of flap-type ailerons at subsonic and transonic speeds.

This paper presents the results of an investigation made on an unswept wing having a modified double-wedge section, an aspect ratio of 2.5, a taper ratio of 0.625, and a 35-percent-chord aileron to determine the effect of fuselage diameter on aileron control, lift, drag, and pitching-moment characteristics. The wing alone and the wing in combination with two different diameter fuselages were investigated. The wing and the wing in combination with the small fuselage were investigated through a Mach number range from 0.60 to 1.18, but the investigation of the wing in combination with the large fuselage was limited to a Mach number range from 0.60 to 1.00.

COEFFICIENTS AND SYMBOLS

C_L lift coefficient $\left(\frac{\text{Twice lift of semispan model}}{qS}\right)$

C_D drag coefficient $\left(\frac{\text{Twice drag of semispan model}}{qS}\right)$

C_m pitching-moment coefficient $\left(\frac{\text{Twice pitching moment of semispan model about } 0.50\bar{c}}{qS\bar{c}}\right)$

C_l rolling-moment coefficient at plane of symmetry $\left(\frac{\text{Rolling moment of semispan model}}{qSb}\right)$

C_{l_a} rolling-moment coefficient produced by deflecting aileron

V stream velocity, feet per second

a velocity of sound, feet per second

M Mach number (V/a)

M_l local Mach number

R Reynolds number of wing based on $\bar{c}$

q dynamic pressure, pounds per square foot $\left(\frac{1}{2}\rho V^2\right)$

ρ mass density of air, slugs per cubic foot

S twice area of semispan wing (including wing area within fuselage), square feet

[redacted]

b twice span of semispan wing, feet

$\bar{c}$ mean aerodynamic chord of wing, 0.276 foot $\left(\frac{2}{S}\int_0^{b/2} c^2 dy\right)$

c local wing chord, feet

y spanwise distance from plane of symmetry, feet

y_i spanwise distance from plane of symmetry to inboard end of aileron, feet

b_a span of aileron measured normal to plane of symmetry, feet

α angle of attack, degrees

δ deflection of aileron relative to wing-chord plane, measured normal to hinge line (positive when trailing edge is down), degrees

$$C_{L_\alpha} = \frac{\partial C_L}{\partial \alpha}$$

$$C_{l_\delta} = \frac{\partial C_l}{\partial \delta}$$

MODEL AND APPARATUS

The steel wing used for this investigation (fig. 1) had an aspect ratio of 2.5, a taper ratio of 0.625, and a 6-percent-thick modified double-wedge airfoil section with the 50-percent-chord line normal to the plane of symmetry.

The two fuselages were modified bodies of revolution having equal lengths but different radii (fig. 2) and were bent to conform to the contour of the bump (figs. 1 and 3).

The wing was used with a root end plate (fig. 1(a)) or with either of the two fuselages (figs. 1(b) and 1(c)) and was mounted in a midwing position with neither incidence nor dihedral. For the wing-fuselage combinations the fuselage was rigidly fastened to the wing and the measured forces therefore included the forces on both wing and fuselage.

A $\frac{1}{32}$-inch-wide slot was cut along the 65-percent-chord line of the wing upper surface approximately three-fourths way through the wing to

[redacted]

form a 35-percent-chord aileron (fig. 3). The various aileron deflections were set by bending the wing trailing edge at the slot and then filling the slot with wax. The aileron extended from the plane of symmetry to the $0.95\frac{b}{2}$ station and was cut into four segments as shown in figure 3. The gaps between undeflected or equally deflected aileron segments were sealed with wax.

TEST TECHNIQUE

The model was tested in the high velocity field of flow over the transonic bump of the Langley high-speed 7- by 10-foot tunnel (fig. 4) through a Mach number range from 0.60 to 1.18. The velocity distribution over the bump in the vicinity of the model is shown in figure 5. The test Mach number was the average Mach number over the span and chord of the wing as determined from plots similar to figure 5. No attempt has been made to take into account the effect of the Mach number gradient over the model.

The forces and moments were measured by an electrical strain-gage balance mounted inside of the bump with the electrical indicator outside of the tunnel test section.

The variation of Reynolds number with Mach number for the investigation is shown in figure 6.

CORRECTIONS

The rolling-moment parameters presented herein represent the aerodynamic effects on a complete wing produced by the deflection of the control on only one semispan of the complete wing. Reflection-plane corrections shown in figure 7 have been applied to the rolling-moment data throughout the Mach range tested. The values given in figure 7 are based on unpublished results of a low-speed experimental investigation in which the aileron effectiveness obtained on complete span wings was compared with that obtained on the same wings tested as semispan models. The corrections obtained by combining these results with theoretical concepts are, therefore, strictly valid only for low Mach numbers; however, it was believed that the results obtained by applying the corrections throughout the Mach number range would give a better representation of true conditions than uncorrected data.

No correction to the rolling moments has been applied for the induced velocity over the end plate. This increment of rolling moment

is believed to be small, probably within the experimental accuracy of the results.

DISCUSSION

The rolling-moment coefficients produced by the aileron for various aileron spans on the wing with the end plate, the small fuselage, and the large fuselage and at various Mach numbers are presented in figures 8 to 11. The rolling-moment-coefficient curves, in general, are linear throughout the deflection range at Mach numbers below approximately 0.90; however, many of the configurations show reduced effectiveness for small aileron deflections at Mach numbers above 0.90.

The variation of rolling-moment coefficient with Mach number (fig. 12) shows the usual decrease of effectiveness with increasing Mach number near $M = 1.0$ but shows no consistent variation of effectiveness with fuselage size. Since the same $0.50\frac{b}{2}$ outboard aileron was used for all three fuselage arrangements, the effectiveness of the control would appear to be practically independent of fuselage diameter within the range investigated. The results indicate, therefore, that in designing controls on similar low-aspect-ratio wings, the wing should be considered as extending through the fuselage. This is further substantiated by the relatively good agreement between the experimental values of C_{l_δ} for the different fuselage configurations at $M = 0.60$ and the estimated values (fig. 13). Since the wing investigated was rather unconventional, further investigations should be made before assuming that the results from this investigation are valid for low-aspect-ratio wing-fuselage combinations in general.

The estimated values of C_{l_δ} were obtained by modifying the method of reference 1 for compressibility effects. The wing plan form was considered as extending to the fuselage center line and was modified by the Glauert-Prandtl transformation (reference 3), and the resulting C'_{l_δ} was modified by the following equation:

$$C_{l_\delta} = \frac{C'_{l_\delta}}{\sqrt{1 - M^2}}$$

where C'_{l_δ} is the aileron-effectiveness parameter estimated by the methods of reference 1 after modifying the wing geometric characteristics by the Glauert-Prandtl transformations.

[redacted]

Adding either of the two fuselages to the wing had only small effects on the lift characteristics of the wing at Mach numbers of 0.60 and 0.90 (fig. 14). Differences in lift-curve slope were found at a Mach number of 0.90, but they were both small and inconsistent. The lift-curve slopes measured at Mach numbers of 0.60 and 0.90 compare favorably with theoretical values estimated by reference 4. (See fig. 15.) As previously mentioned, further investigations should be made with more conventional wings to verify these results.

The increase in drag coefficient caused by the fuselage is about four times as great for the large fuselage as for the small fuselage at $M = 0.60$ (fig. 14). This increase is of the correct order of magnitude as the large fuselage has twice the diameter of the small fuselage. The increments in drag at 0.90 appear low and probably result from a forward motion of a region of separated flow on the bump as the Mach number was increased from 0.60 to 0.90. The resulting pressure gradient over the fuselage could result in a thrust effect on the fuselage. Although this condition may exist, it is believed that it has a negligible effect on the lift and pitching-moment coefficients at low and moderate angles of attack.

The expected decrease in the stability of the combination (that is, C_m/C_L became more positive) resulted from adding the fuselage to the wing. The effect of the large fuselage was about four times that of the small fuselage in this respect.

CONCLUSIONS

An investigation was made at subsonic and transonic speeds to determine the effects of fuselage diameter on some of the aerodynamic characteristics of a wing having a modified double-wedge section, an aspect ratio of 2.5, a taper ratio of 0.625, an unswept 50-percent-chord line, and a 35-percent-chord aileron of various spans. The following conclusions were indicated:

1. The wing lift-curve slope was only slightly affected by the addition of a fuselage the diameter of which was less than 40 percent of the wing span.

2. Aileron effectiveness at zero angle of attack was not appreciably affected by the fuselage diameter when the fuselage diameter was not more than 40 percent of the wing span.

Langley Aeronautical Laboratory
National Advisory Committee for Aeronautics
Langley Air Force Base, Va.

REFERENCES

1. Lowry, John G., and Schneiter, Leslie E.: Estimation of Effectiveness of Flap-Type Controls on Sweptback Wings. NACA TN 1674, 1948.

2. DeYoung, John: Spanwise Loading for Wings and Control Surfaces of Low Aspect Ratio. NACA TN 2011, 1950.

3. Göthert, B.: Plane and Three-Dimensional Flow at High Subsonic Speeds. NACA TM 1105, 1946.

4. DeYoung, John: Theoretical Additional Span Loading Characteristics of Wings with Arbitrary Sweep, Aspect Ratio, and Taper Ratio. NACA TN 1491, 1947.

[redacted]

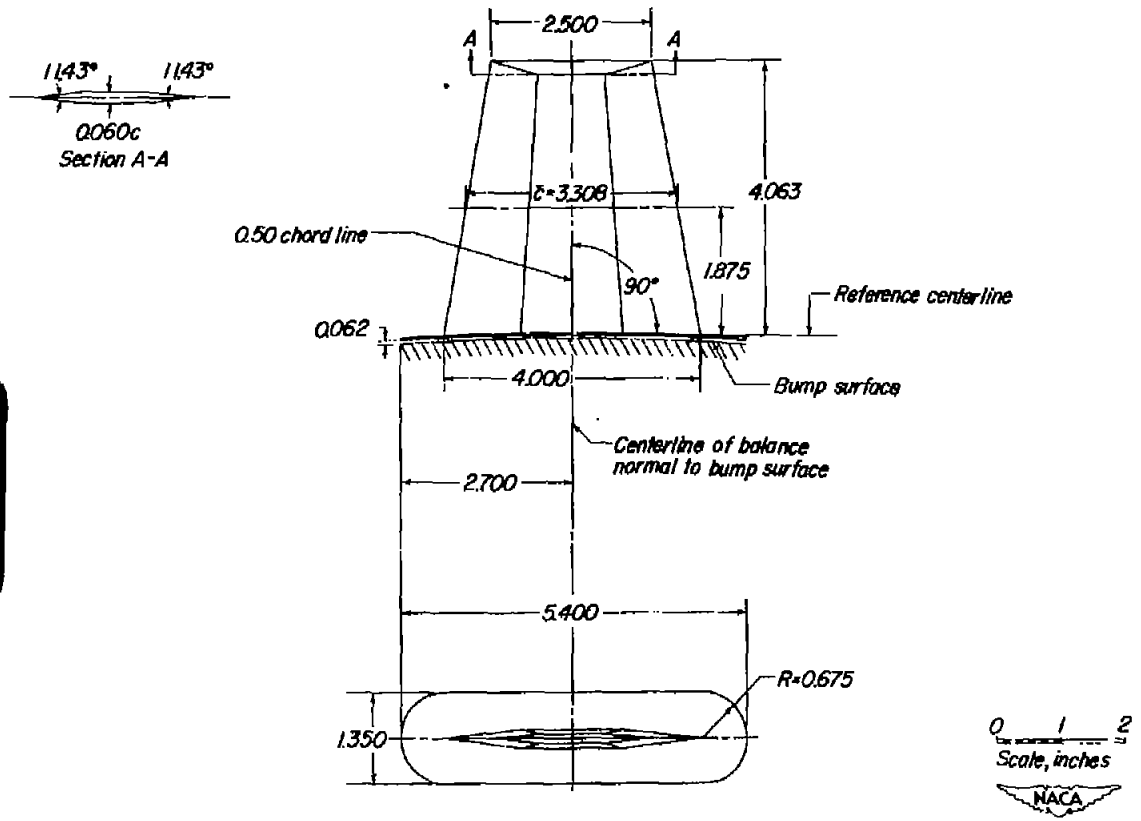

Tabulated Wing Data

Area (Twice semispan)	0.1834 sq ft
Mean aerodynamic chord	0.276 ft
Aspect ratio	2.500
Taper ratio	0.625
Incidence	0.0°
Dihedral	0.0°

(a) Model wing with end plate.

Figure 1.- Geometric characteristics of the 6-percent-thick modified double-wedge wing.

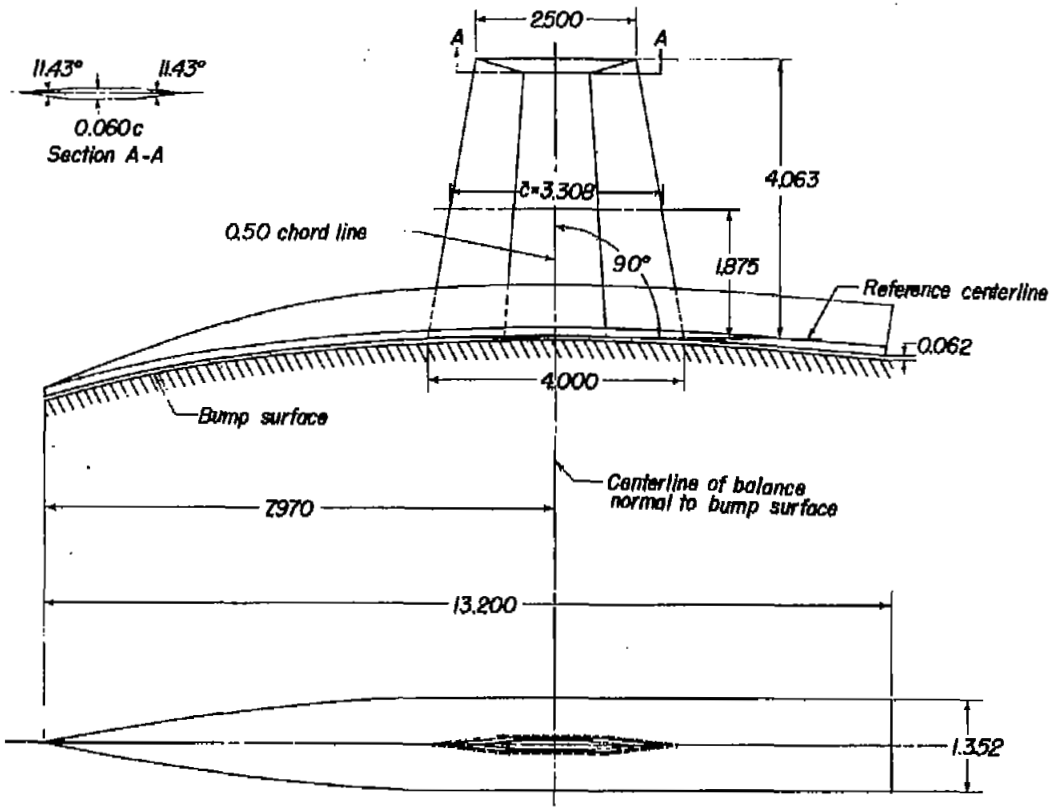

Tabulated Wing Data

Area (Twice semispan)	0.1834 sq ft
Mean aerodynamic chord	0.276 ft
Aspect ratio	2.500
Taper ratio	0.625
Incidence	0.0°
Dihedral	0.0°

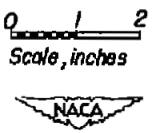

(b) Model wing with small fuselage.

Figure 1.- Continued.

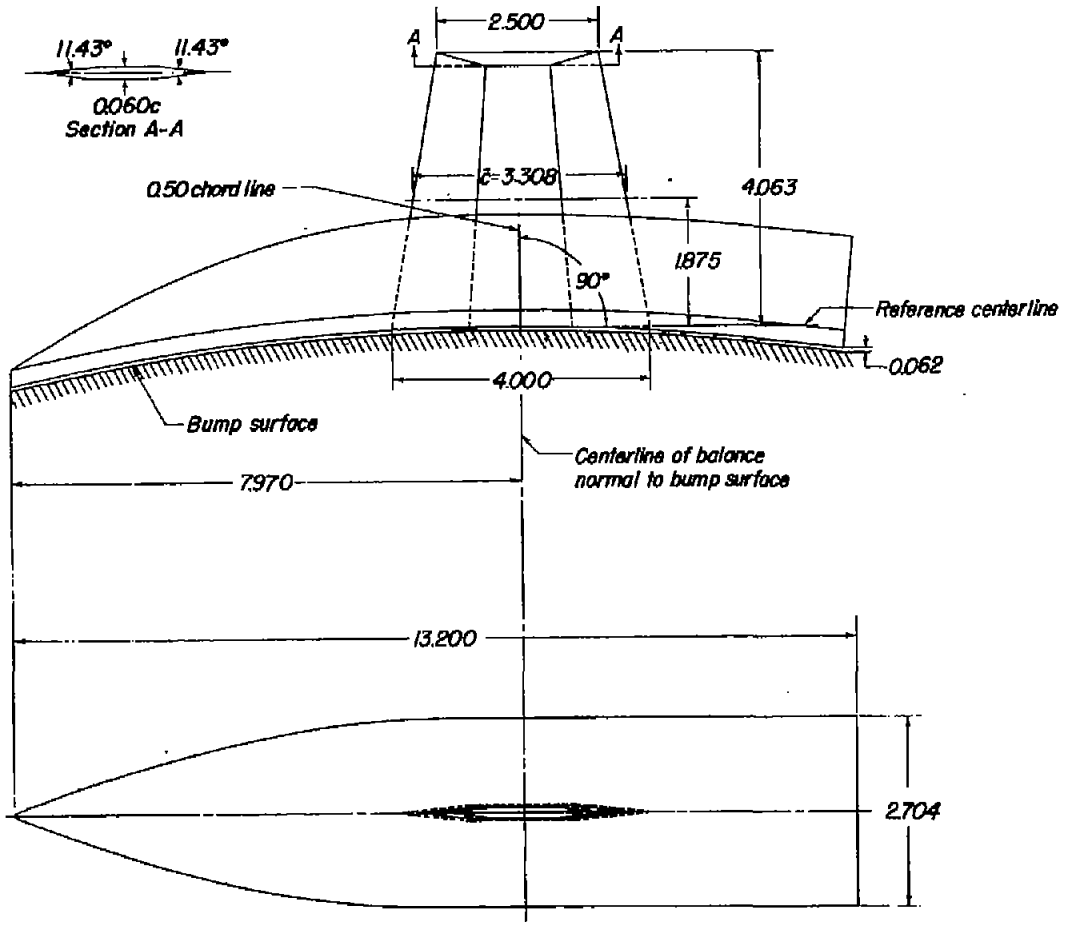

Tabulated Wing Data

Area (twice semispan)	0.1834 sq ft
Mean aerodynamic chord	0.276 ft
Aspect ratio	2.500
Taper ratio	0.625
Incidence	0.0°
Dihedral	0.0°

(c) Model wing with large fuselage.

Figure 1.- Concluded.

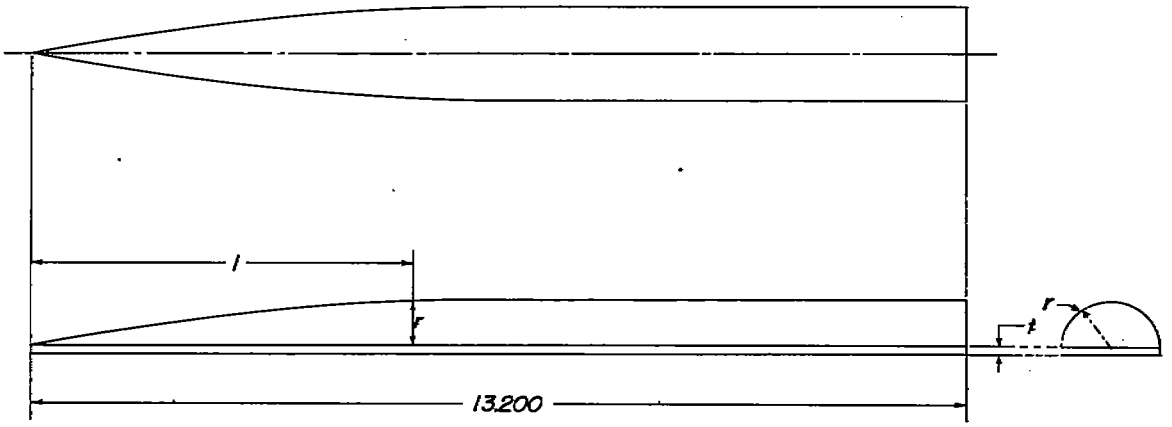

Small fuselage ordinates, inches	
l	r
0	0
0.676	0.117
1.353	.225
2.029	.325
2.706	.413
3.382	.489
4.059	.555
4.735	.613
5.412	.649
6.088	.672
6.765	.676
13.200	.676
t = 1/8"	

Large fuselage ordinates, inches	
l	r
0	0
0.676	0.234
1.353	.450
2.029	.650
2.706	.826
3.382	.978
4.059	1.110
4.735	1.226
5.412	1.298
6.088	1.344
6.765	1.352
13.200	1.352
t = 1/4"	

Figure 2.- Drawing and ordinates of the fuselages.

[redacted]

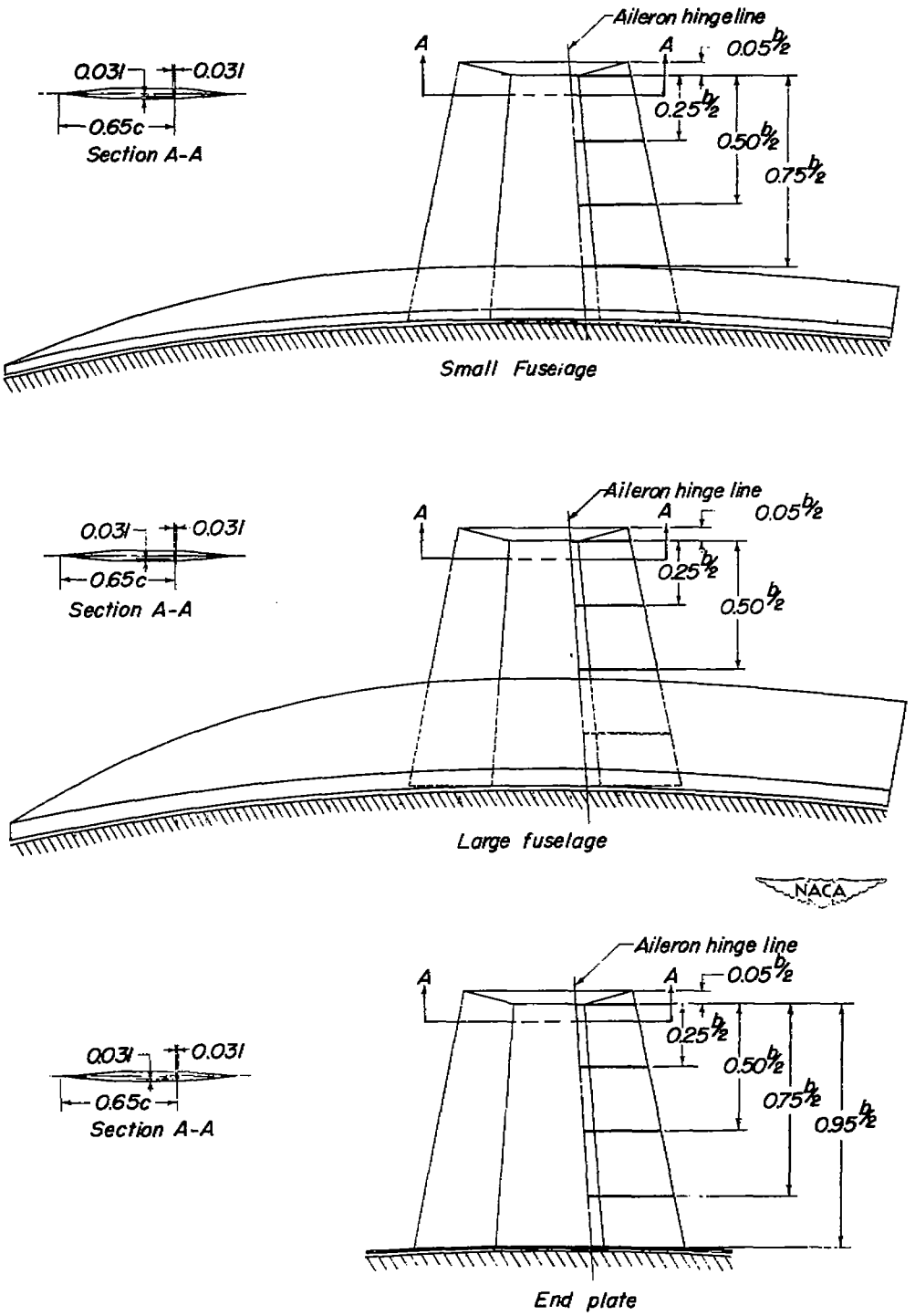

Figure 3.- Details of ailerons tested with the end plate and fuselages.

[redacted]

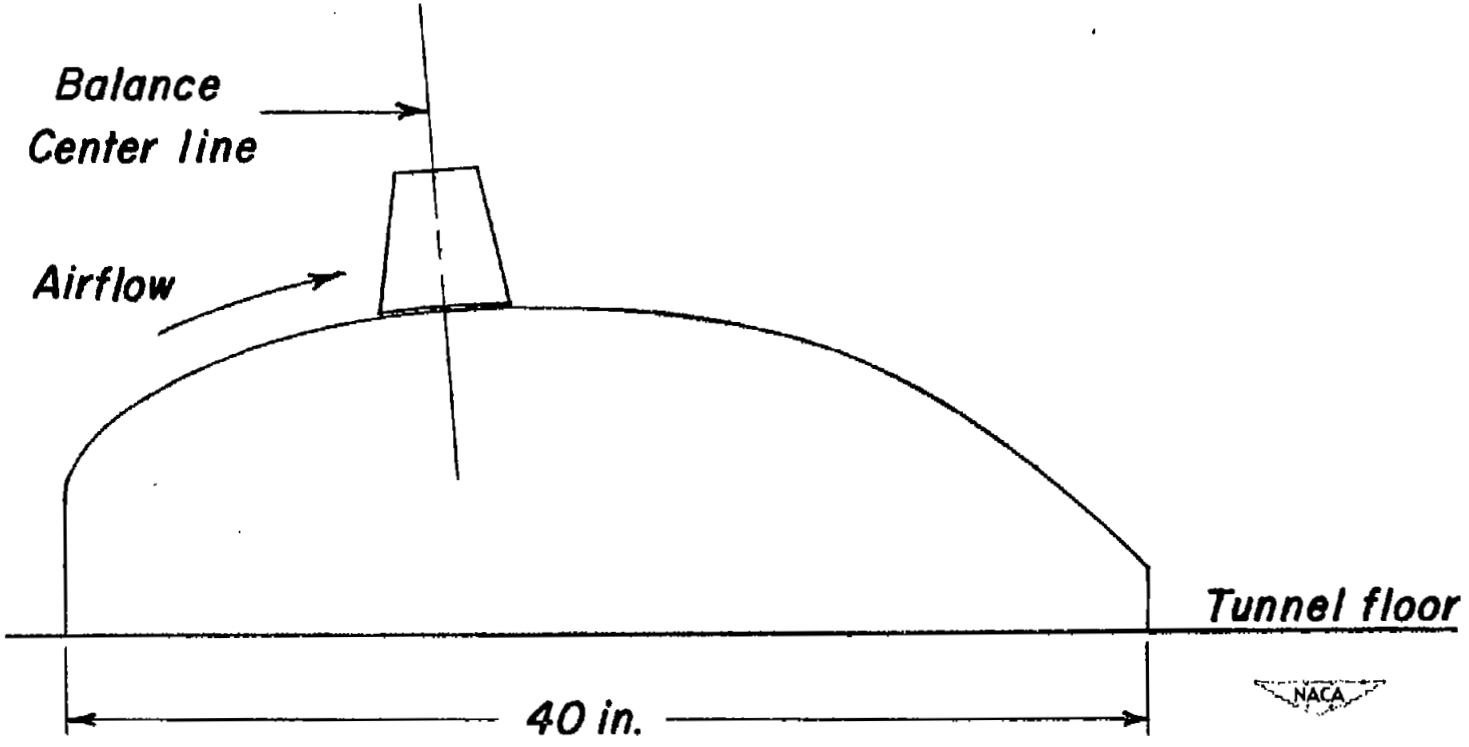

Figure 4.- Schematic sketch of relative position of model, balance, and transonic bump as mounted in the Langley high-speed 7- by 10-foot tunnel.

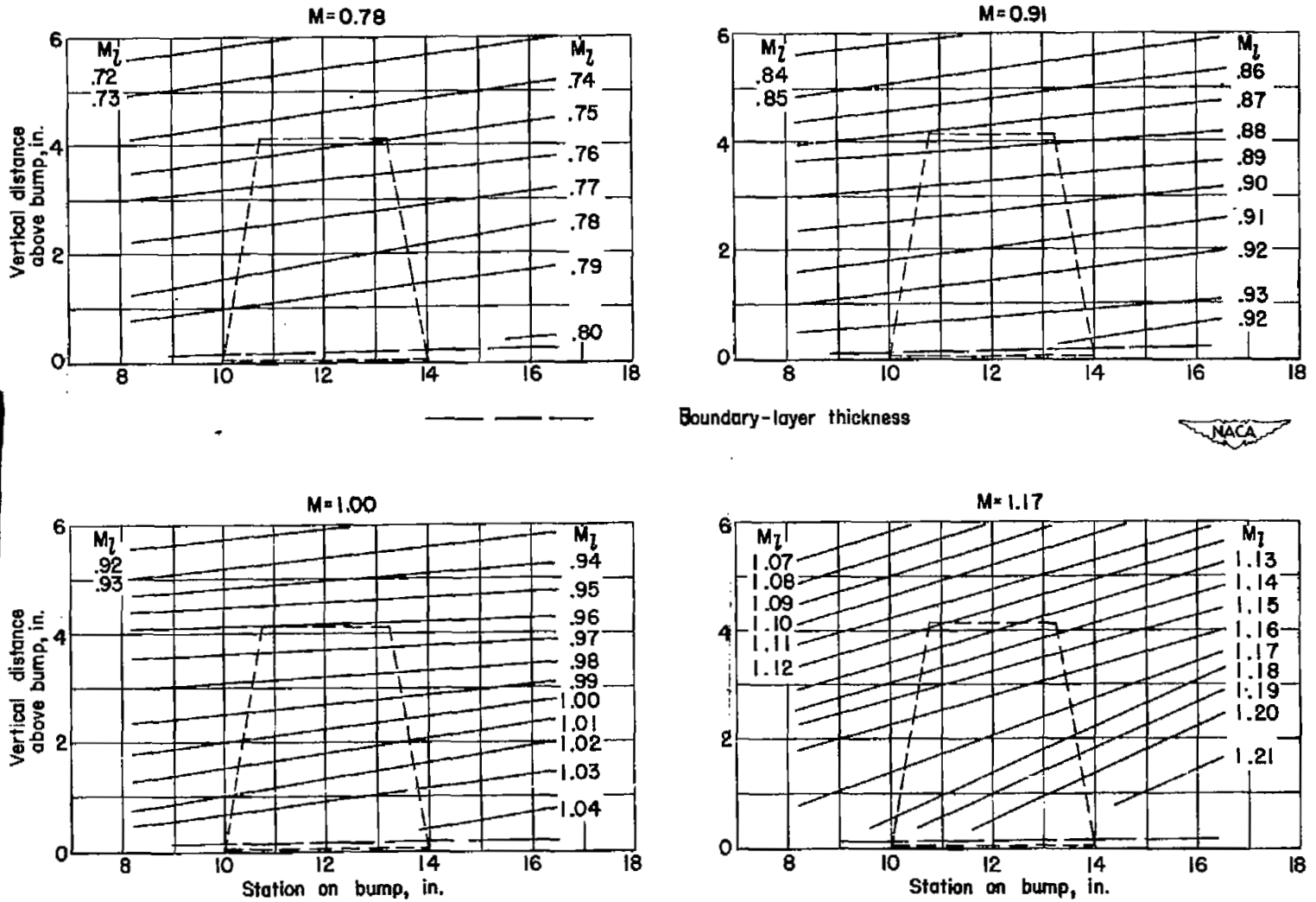

Figure 5.- Typical Mach number contours over transonic bump in region of model location.

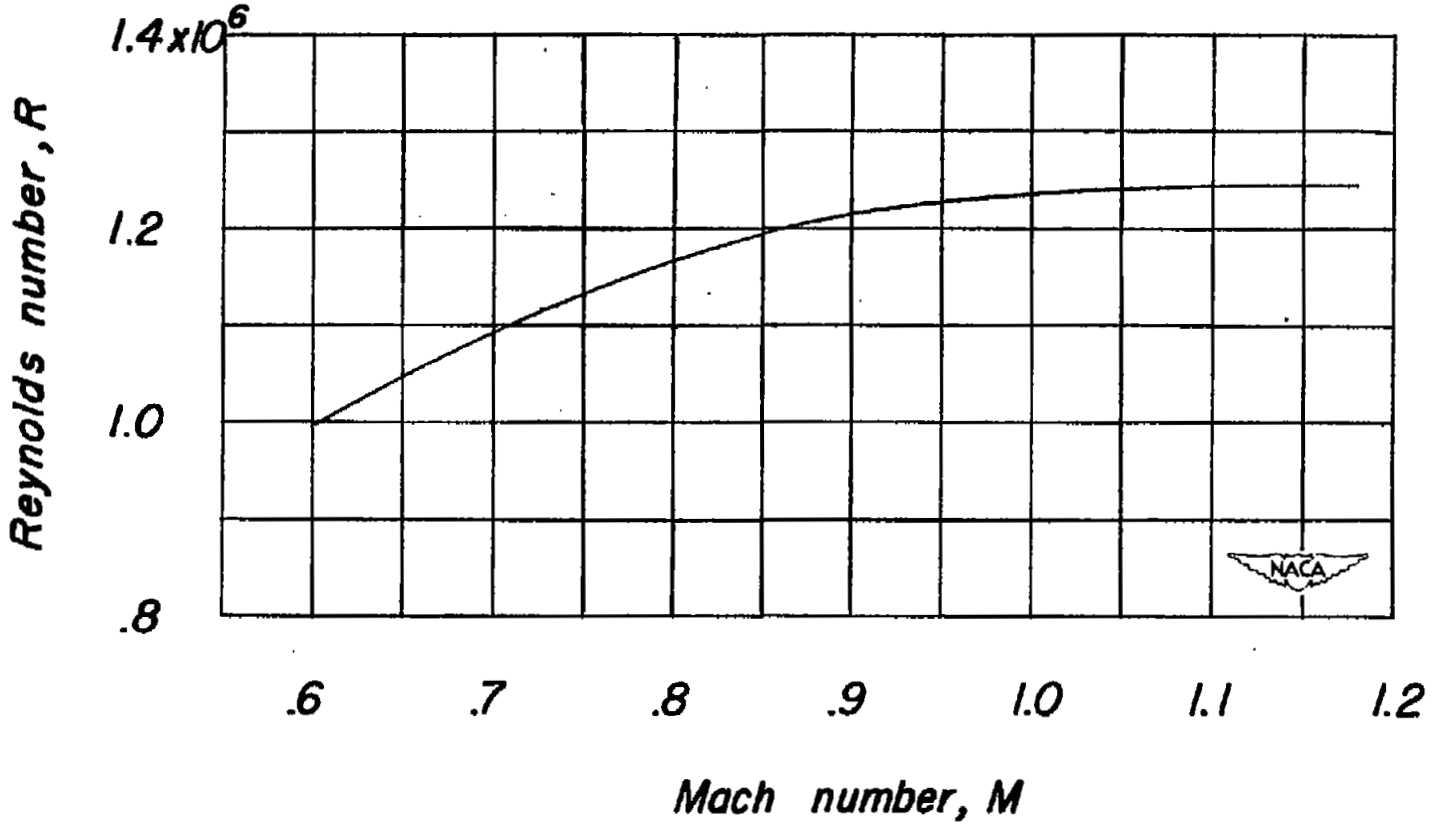

Figure 6.- Variation of mean test Reynolds number with Mach number.

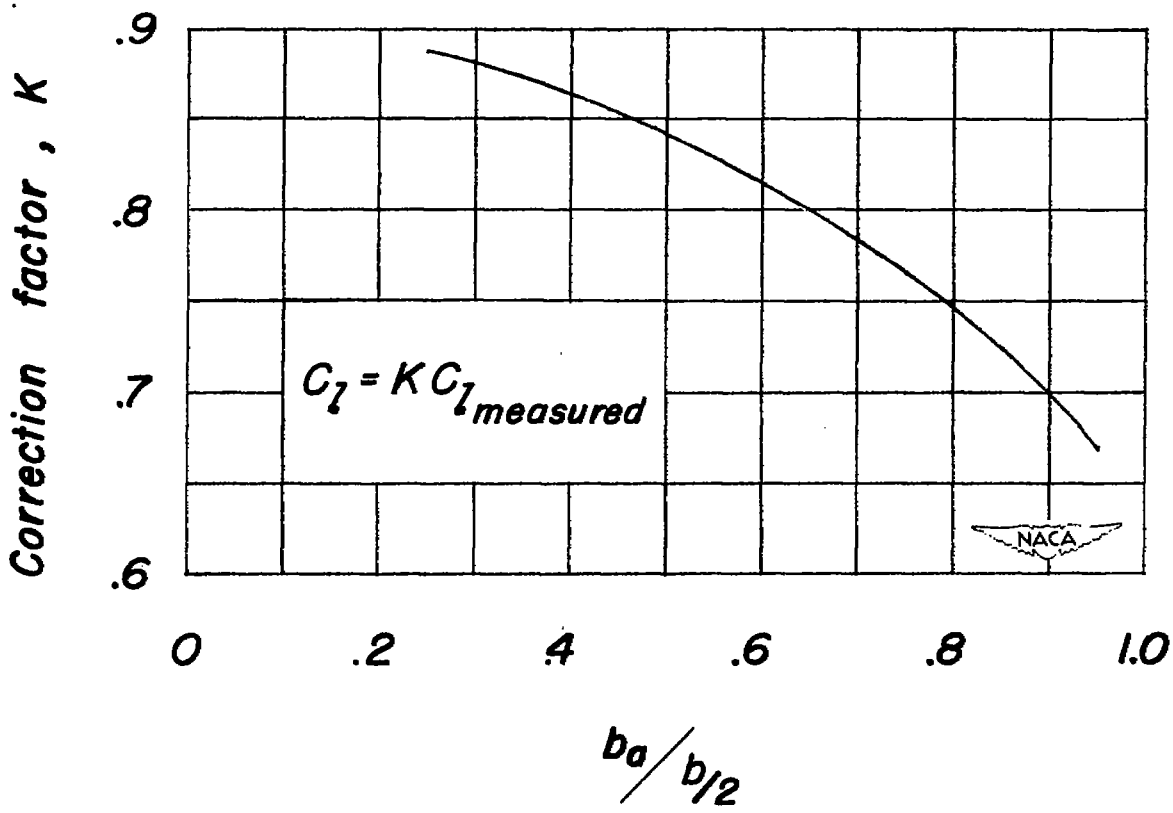

Figure 7.- Reflection-plane correction factors for outboard ailerons of various spans for a unswept wing having an aspect ratio 2.5 and taper ratio 0.625.

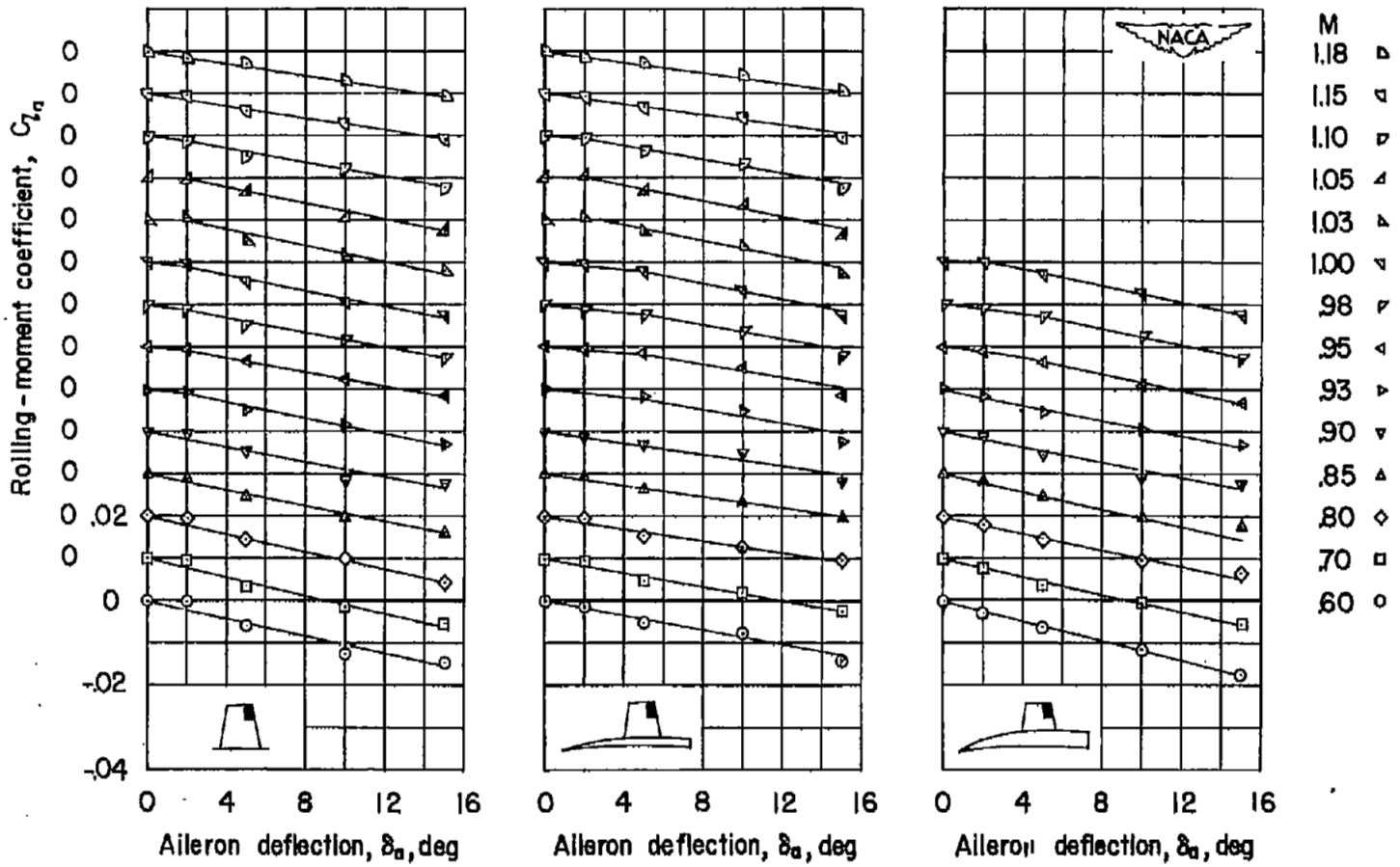

(a) End plate. (b) Small fuselage. (c) Large fuselage.

Figure 8.- Variation of rolling-moment coefficient with aileron deflection for various Mach numbers. $b_a = 0.25\frac{b}{2}$, $y_i = 0.70\frac{b}{2}$, $\alpha = 0^\circ$.

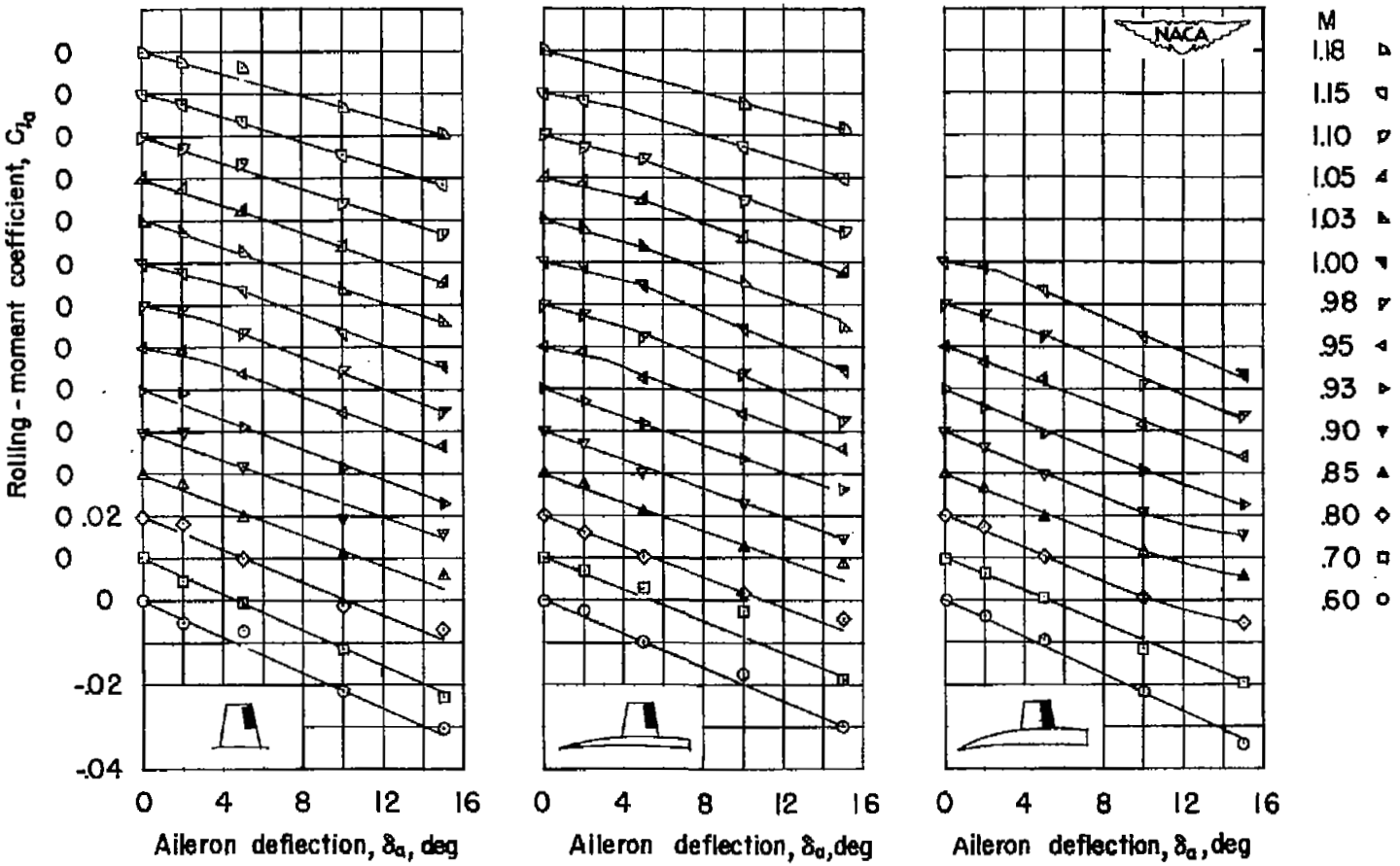

(a) End plate. (b) Small fuselage. (c) Large fuselage.

Figure 9.- Variation of rolling-moment coefficient with aileron deflection for various Mach numbers. $b_a = 0.50\frac{b}{2}$, $y_i = 0.45\frac{b}{2}$, $\alpha = 0^\circ$.

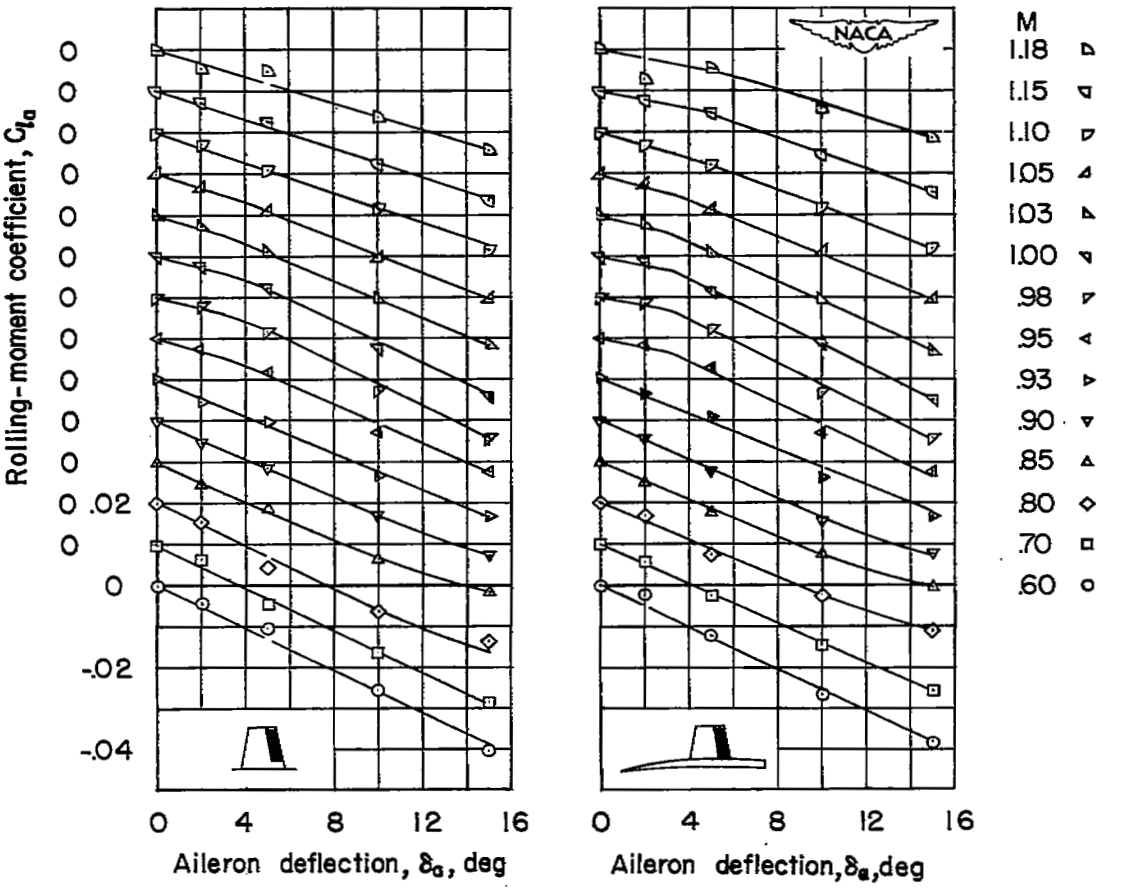

(a) End plate. (b) Small fuselage.

Figure 10.- Variation of rolling-moment coefficient with aileron deflection for various Mach numbers. $b_a = 0.75\frac{b}{2}$, $y_i = 0.20\frac{b}{2}$, $\alpha = 0^\circ$.

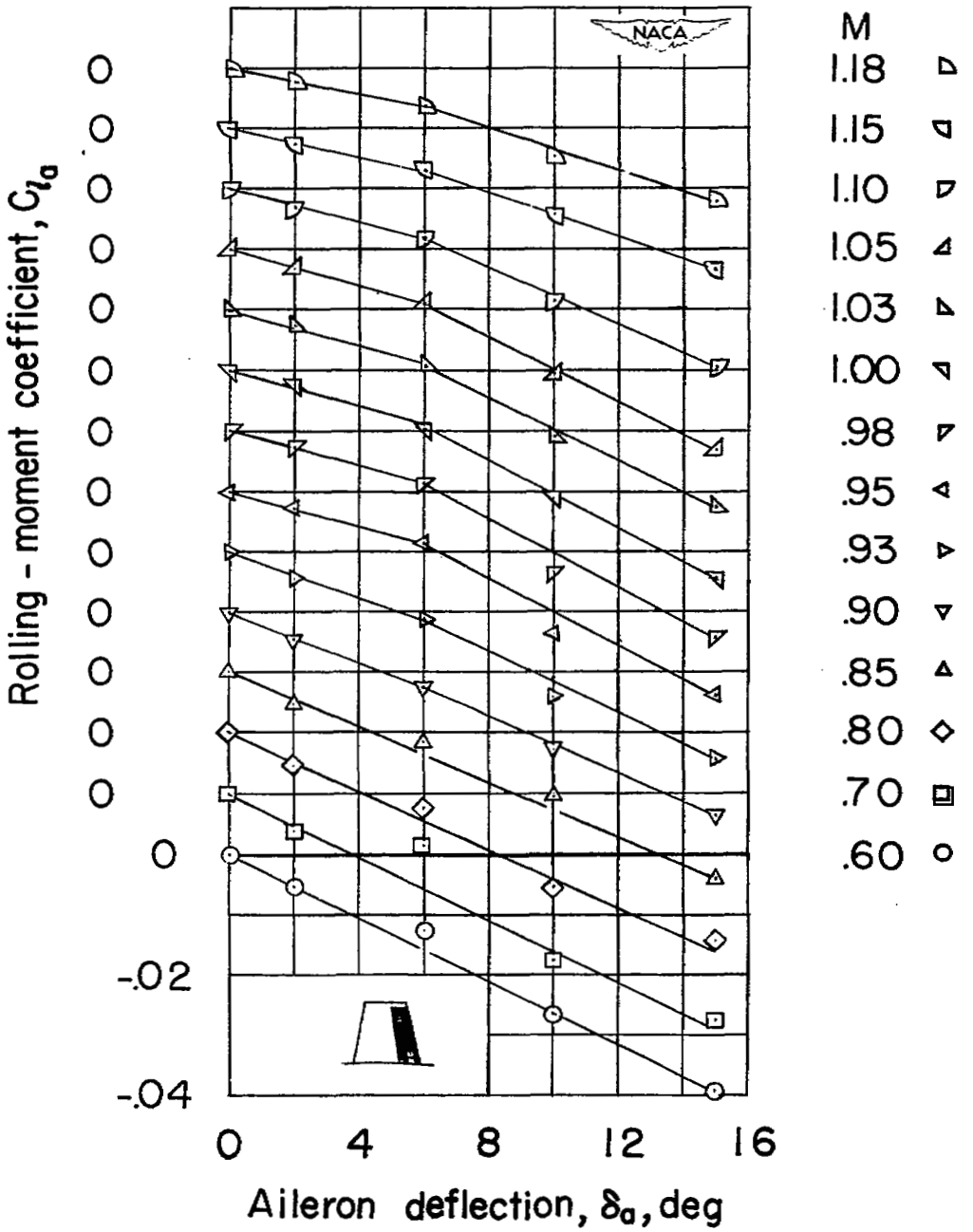

Figure 11.- Variation of rolling-moment coefficient with aileron deflection for various Mach numbers. $b_a = 0.95\frac{b}{2}$, $y_i = 0.00\frac{b}{2}$, $\alpha = 0^\circ$.

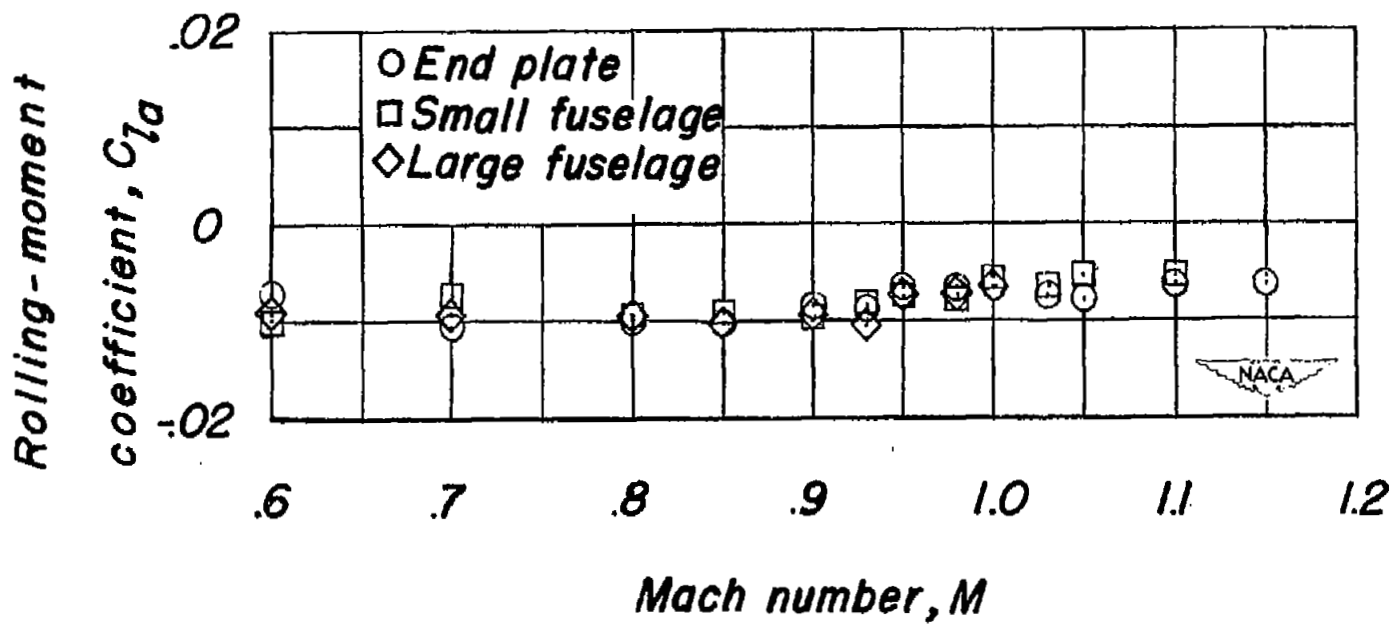

Figure 12.- Variation of rolling-moment coefficient with Mach number, $b_a = 0.50\frac{b}{2}$, $y_j = 0.45\frac{b}{2}$, $\alpha = 0^\circ$, $\delta = 5^\circ$.

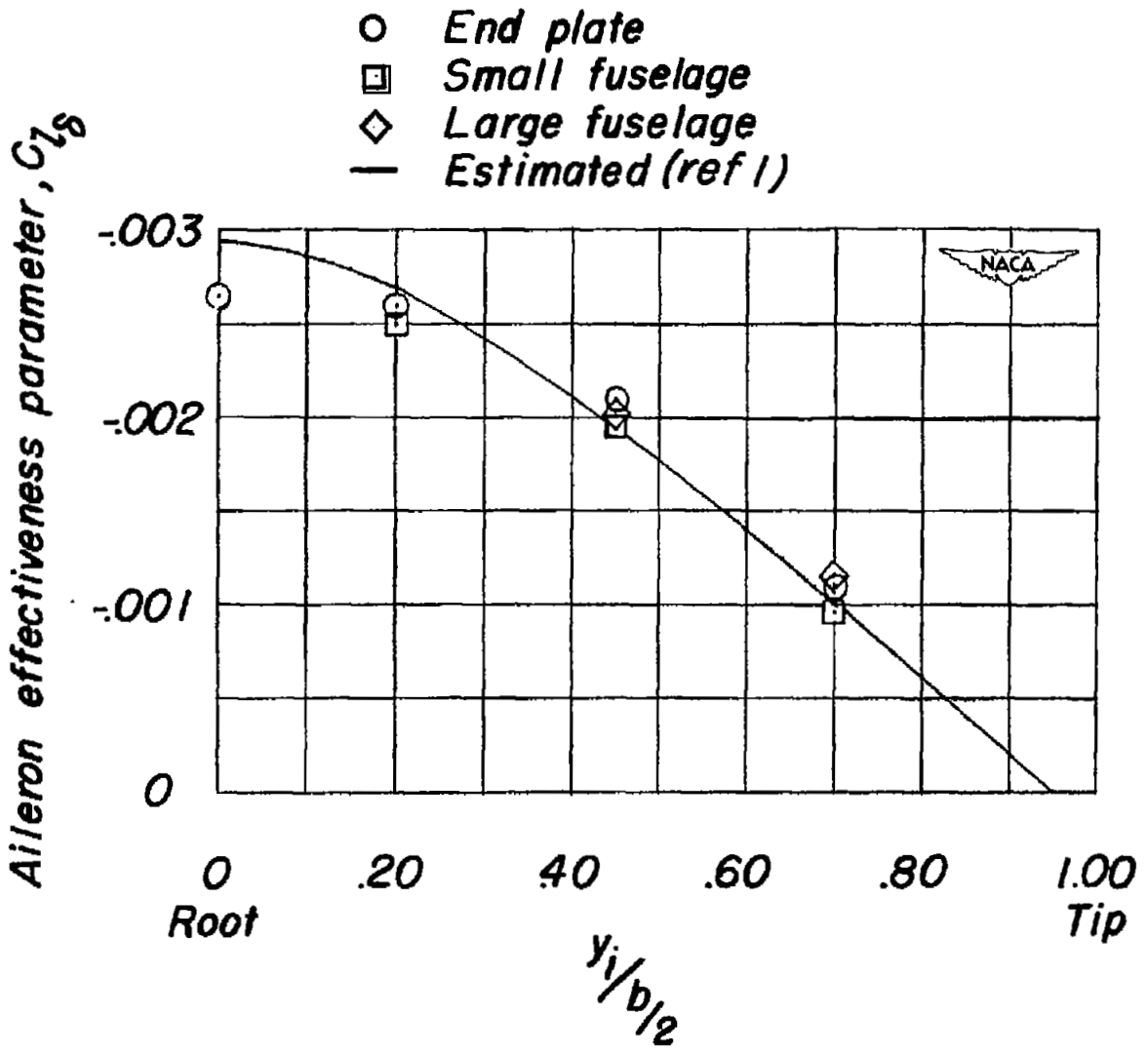

Figure 13.- Variation of aileron-effectiveness with control span.
M = 0.60; $\alpha = 0^\circ$.

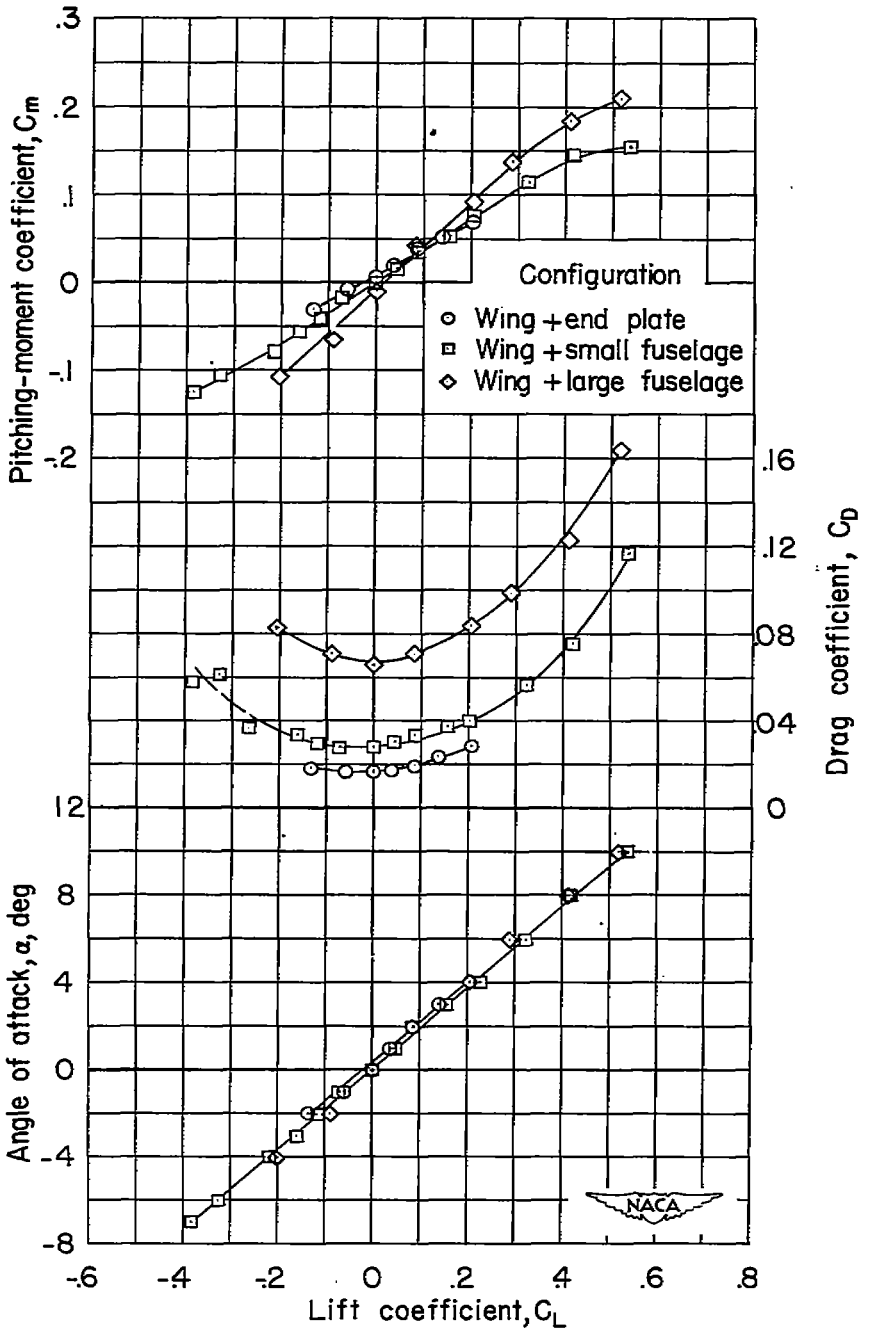

(a) M = 0.60.

Figure 14.- Aerodynamic characteristics of the 6-percent-thick modified double-wedge wing with unswept 50-percent chord line, aspect ratio 2.50, and taper ratio 0.625. $\delta = 0^\circ$.

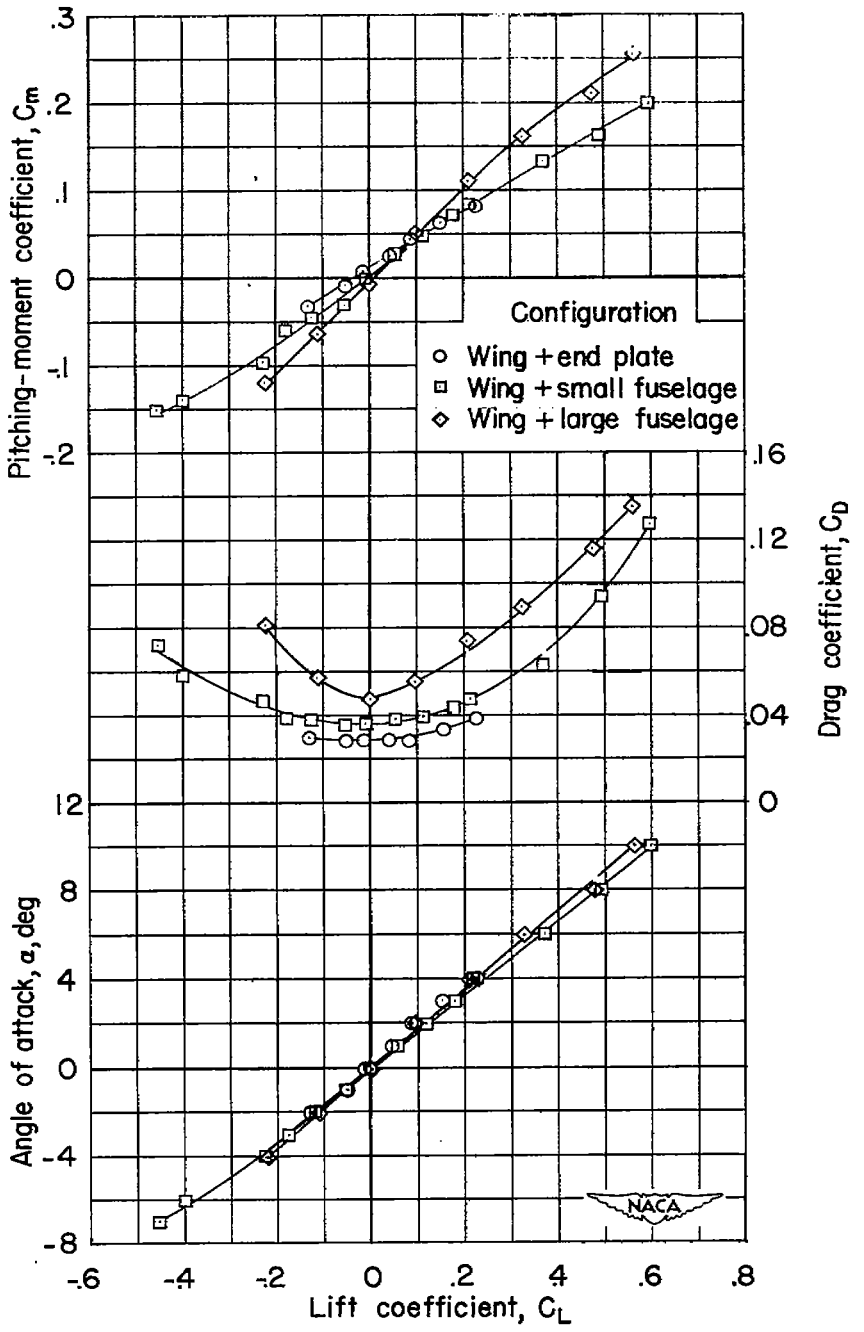

(b) M = 0.90.

Figure 14.- Concluded.

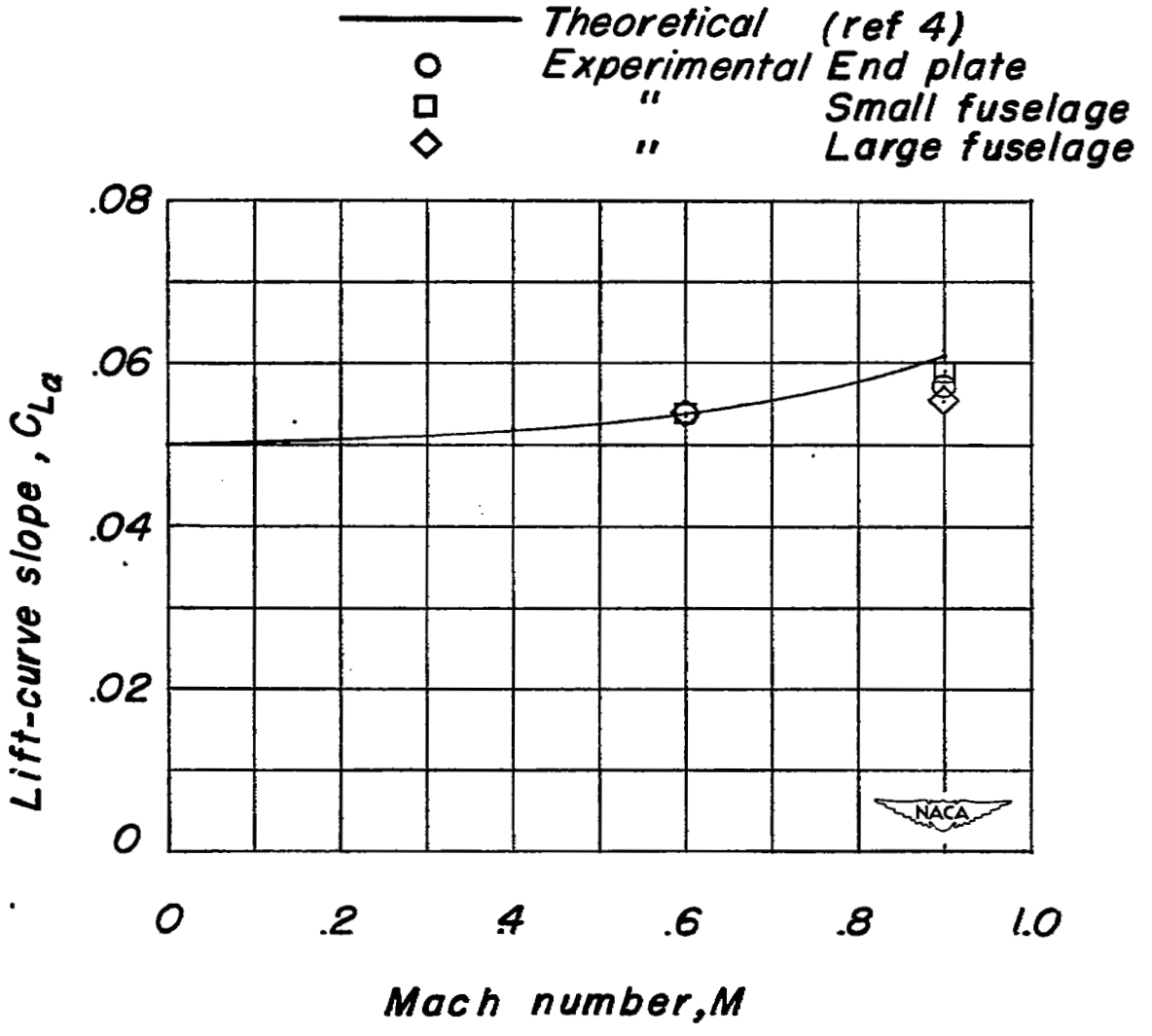

Figure 15.- Variation of lift-curve slope with Mach number for an aspect ratio 2.5 wing.